SPACE TELESCOPE SCIENCE INSTITUTE
Operated for NASA by AURA

WFC3 Instrument Science Report 2013-07

Characterizing Persistence in the WFC3 IR Channel: Observations of Omega Cen

Knox S. Long, Sylvia Baggett & John W. MacKenty
July 9, 2013

ABSTRACT

The HgCdTe IR array detector that is the heart of the IR channel of WFC3 exhibits persistence effects, after-images lasting more than an orbit due to bright objects in earlier exposures, that need to be considered in the analysis of IR data. The amount of persistence is primarily a function of the maximum degree of saturation within the earlier exposures and the time since those exposures. However, it also depends on the entire exposure history. Here we describe a series of calibration observations involving relatively dense star fields in the globular cluster Omega Cen designed to aid in characterizing how exposure history affects the amount of persistence. These observations consisted of one or more non-dithered exposures of Omega Cen followed by a series of darks. We show that the amplitude of persistence increases by about 25% after 6 identical multi-accum exposures, each lasting 349 s, compared to a single exposure. The exponent of the power law decay of the persistence flattens somewhat, indicating that persistence also lasts for a longer period of time after repeat exposures. We use these data to better characterize how persistence varies with fluence, the effective number of electrons deposited on a pixel in an exposure. Finally, in the context of the current consensus model for persistence in IR arrays involving traps within the depletion region of the diodes that constitute the pixels, we estimate the effective number of traps involved in persistence in the WFC3 IR detector.

Introduction

The WFC3 IR HgCdTe Hawaii 1R detector on HST has performed extremely well on orbit. However, it does exhibit an anomaly, persistence, that is characteristic of all such IR arrays. Persistence manifests itself as ghost images or afterglow from earlier

exposures containing sources that saturate or nearly saturate the pixels. Persistence is large enough and lasts long enough to be of concern for some scientific observations. As a result, a vigorous calibration program has been carried out to characterize persistence in the WFC3 IR channel.

We have used results from earlier phases of this program to develop an initial model of persistence in the IR detector of WFC3 (Long et al. 2012).[1] The model characterizes persistence in each pixel in terms of the time since an earlier exposure and the fluence reached in that pixel in that exposure. As currently implemented, fluence is calculated as the total number of electrons measured in the "flt" file of the earlier exposure. The functional form of our initial model is as follows:

$$P_{ij} = A_{ij} \left(\frac{1}{e^{\frac{x-x_o}{\delta x}} + 1} \right) \left(\frac{x}{x_o} \right)^{\alpha} \left(\frac{t}{1000\ s} \right)^{-\gamma}, \quad (1)$$

where P_{ij} is the persistence at time t after the end of an exposure with a fluence level of x. The first term A_{ij} in this equation describes a spatially dependent normalization, while the second term is a Fermi-like distribution that describes the rapid rise in persistence near saturation in terms of a characteristic fluence x_o and width δx. The third term in the equation describes a slow rise in persistence (generated by very high fluences) in terms of a power law with exponent α, while the fourth describes the decay with time in terms of a power law with exponent γ. If there are multiple exposures that could cause persistence, the initial model counts only the exposure that would cause the most persistence in the current image.

The model of persistence that we use is loosely based on the accepted physical model for persistence in IR arrays (Smith et al. 2008ab), which explains the effect as arising from dislocations in the depletion region of reversed-biased diodes that constitute the pixels of an IR array. Voltage levels within the diode change as the reverse bias of the diode decreases during the course of a multi-accum exposure, exposing portions of the depletion region to free charge. Dislocations in these newly exposed regions trap charge. More traps are exposed for bright sources than for faint ones. This trapped charge is released in later exposures, resulting in after-images.

In the context of this trap and release model, our description of persistence implicitly assumes that trapping times are short, so that all of the exposed traps are filled at the end of an exposure. If that is not the case, then persistence will not be simply a function of the maximum fluence level, but rather of the entire exposure history of a pixel. Experience with other similar IR detectors suggests that trapping times are, in fact, important, and therefore we have begun to characterize its effects on the detector that is part of the WFC3 IR channel.

[1] In Long et al. (2012), we described a slightly different version of this equation, such that the normalization was effectively the amplitude of the persistence at x_o at 1000 s. However the software that we are using to estimate the amount of persistence in HST images uses the equation described here, without a factor of 2 in the numerator of the second term. In this case, the amplitude is a characteristic amplitude at 1000 s at a few times saturation.

Table 1. Visits with Persistence Model Fits

Visit	Dataset	Obs. Date	A ($e\ s^{-1}$)	x_o (e)	δx (e)	α	γ	Pre-dark ($e\ s^{-1}$)
11	ibvd11aaq	2/27/12 03:01	0.344	86738	18212	0.144	1.019	-0.001
31	ibvd31vuq	4/27/12 20:18	0.343	86516	17774	0.146	1.021	-0.004
22	ibvd22n1q	4/15/12 05:02	0.398	83663	18318	0.137	0.966	0.013
13	ibvd13ihq	3/19/12 19:15	0.389	84236	18874	0.159	0.952	0.015
33	ibvd33sdq	3/20/12 20:47	0.398	83627	19395	0.151	0.946	0.009
24	ibvd24idq	3/17/12 20:58	0.395	85278	19424	0.157	0.945	0.025
15	ibvd15c6q	4/28/12 20:27	0.421	82011	19191	0.153	0.914	0.014
35	ibvd35maq	3/03/12 04:19	0.437	80520	18872	0.148	0.904	-0.001
26	ibvd26qqq	3/20/12 16:00	0.426	82116	19645	0.152	0.911	0.010

Here we describe one series of tests in which multiple observations of three regions of the globular cluster Omega Cen were made to explore the effects of differing numbers of multiaccum exposures on persistence. Another test involving internal flats has been described by Long & Baggett (2013).

Observations

The data for this program (Prop. ID 12694) comprised nine separate visits, which were executed between February and April of 2012. Each visit consisted of an initial dark exposure, one or more non-dithered multi-accum exposures of a portion of Omega Cen, and a series of follow-on darks. The purpose of the initial dark was to verify that the detector was in a normal state at the beginning of the visit. The Omega Cen exposures were all multiaccum exposures (STEP50 with NSAMP of 13) taken with the F125W filter; each exposure lasted 349 s. The number of repeats varied from one to six. Three separate regions of Omega Cen were observed. A summary of the observations, ordered by the number of repeats, is presented in Table 1 along with other information that will be discussed further below. The visit numbers have a specific nomenclature pertaining to the Omega Cen exposure(s), with the first digit indicating which of the three positions was observed and the second digit indicating the number of repeats. For this report, all of the data have been re-reduced with version 3.1.2(11-Feb-2013) of the CALWF3 pipeline. Calibration keywords were all set to PERFORM so that all of the data, including darks, was processed as if they were normal on-sky observations. A dummy flat (PFLTFILE) with all values set to unity was utilized.

For the analysis described here, we are primarily concerned with the average properties of the detector. Unless otherwise indicated, the values represent averages or medians of "good pixels" as defined by data quality flags in the processed (flt) files.

All of the pre-darks for visits in this program were nominal. The median values of the pre-darks after processing are given in Table 1. We also used our current version of persistence subtraction software to check whether there should have been persistence due to earlier exposures. Little or no persistence was predicted.

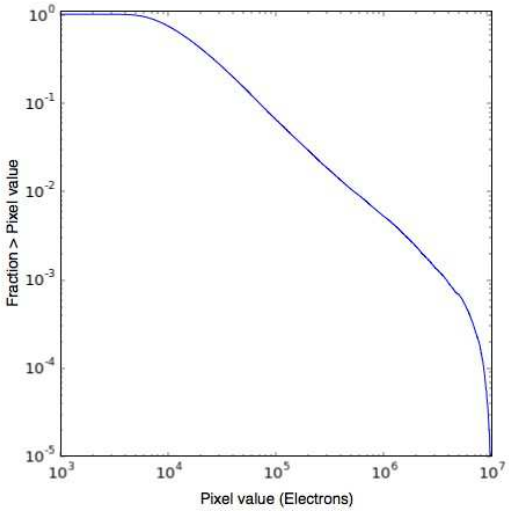

Figure 1. The fraction of pixels with fluences exceeding a given value in the Omega Cen exposure in Visit 11. All three positions observed produce very similar distributions of pixel values.

The Omega Cen exposures were designed on the one hand to contain a large number of stars of sufficient brightness to generate persistence and on the other hand to leave enough area with low fluence so that background in the darks could be measured reliably. The cumulative distribution of fluences in the Omega Cen exposure from Visit 11 is shown in Figure 1. About 22% and 10% of the pixels in this image reached half and full saturation, respectively, where saturation is taken to be 70,000 electrons. On the other hand, 30% of pixels have fluence levels less than 10,000 electrons, where persistence is known to be a relatively small effect. The distribution of fluences at position 1 (in Visit 11) is similar to that obtained at the two other positions that were observed with WFC3 in this program. Bright stars are scattered fairly uniformly across the IR images, without strong gradients. As a result of the point spread function associated with HST and WFC3, each bright star produces pixels in close proximity to one another with a range of fluence levels.

A "dark" image taken shortly after the Omega Cen exposure in Visit 11 is shown in Figure 2. It looks very similar to the original Omega Cen exposure (when the original exposure is displayed with a stretch that emphasizes the brighter objects).

To determine the "average" persistence in this and other "dark" exposures, we adopted the following binning procedure: We first identified all pixels in the Omega Cen exposure that had the same fluence, binned in intervals that varied from 1000 to 10,000 electrons depending on the fluence level. We then calculated raw values of the persistence from the same pixels in the "dark" exposure. In creating "flt" files, the CALWF3 pipeline removes an estimate of the average dark current. However, the dark current in the IR detector is variable; Hilbert & Petro (2012) estimate the variations to

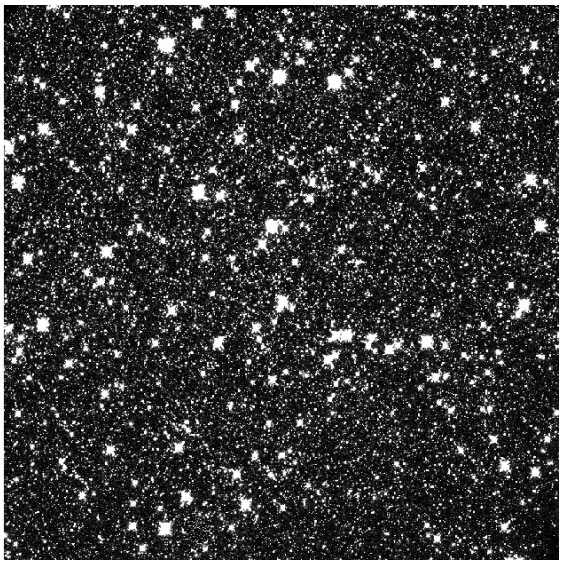

Figure 2. The first dark after the Omega Cen exposure from Visit 11 displayed on a linear scale from 0 to 0.5 e s^{-1}. The dark exposure began 230 s after the end of the Omega Cen exposure.

be of order 16% of the average dark current or 0.0075 e s^{-1}. Therefore, to minimize the effect of these dark current variations in the "dark" images, we identified all of the pixels in the Omega Cen exposure with fluence levels levels between 1000 and 5000 electrons, and assumed these provided a good measure of the residual dark current in that image. We subtracted this from the raw value of the persistence. In all of these calculations, we used median values of pixels, excluding from consideration any pixel with the data quality flag set to a non-zero value.

The average persistence as a function of fluence resulting from one of the Omega Cen exposures, Visit 11 specifically, is shown in Figure 3, plotted both on log-linear and log-log scales. Each of the curves represents the level of persistence in a different dark sequence taken after the Omega Cen exposure. The first dark (blue in Figure 3) was obtained about 230 s after the end of the Omega Cen exposure; the last dark (purple) was about 6,300 s after the end. As one can see, to first order, the shape of the persistence remains the same with time while the overall amplitude simply decreases. This behavior is part of the justification for the separation of time and fluence in our initial model of persistence in the WFC3/IR channel. The log-log plot makes it clear that while persistence is small below fluence levels of about half saturation, it does exist at low levels down to fluence levels below 10,000 electrons. For comparison purposes, we note that the mean dark current for the WFC3 IR array is 0.046 e s^{-1} (Hilbert & Petro 2012).

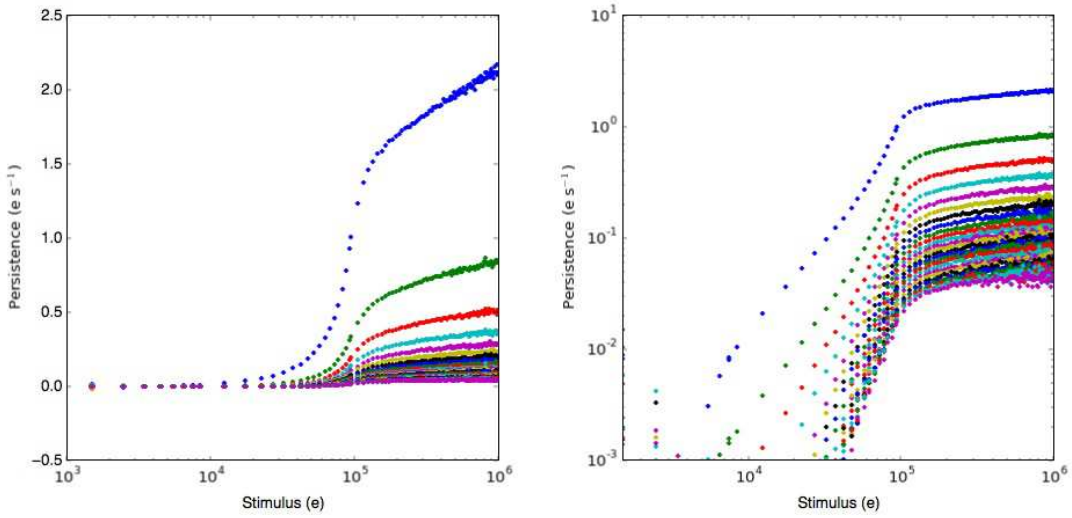

Figure 3. Persistence as a function of stimulus on log-linear (left) and log-log (right) scales in each of the darks after the Omega Cen exposure in Visit 11. Dark current for these figures was estimated from regions of the detector in which fluence in the Omega Cen exposure was between 1000 and 5000 e.

Analysis

The purpose of this calibration program was to determine how sensitive persistence is to the exposure history of a pixel as opposed simply to the maximum fluence level. That the exposure history is important is straightforward to demonstrate from these data. As an initial indication, we simply fit the persistence from each of the visits to the formula we used for our current characterization of persistence. The quality of the fit is indicated in Figure 4 (data are in blue, model is in green). In general, the data are fit quite well, with the possible exception of the "knee" in the curve, where there is less persistence than the model predicts. While this may be due in part to the fact that our Fermi-like function simply does not reflect the shape of the persistence curve, it is also apparent that persistence decays more rapidly here than for very high fluence levels, a fact we shall return to later.

The results of the fits for all the visits are listed in Table 1. There are significant differences in some of the fitted parameters in observations with different numbers of repeats. In particular, as shown in Figure 5, the amplitude A_{ij} rises by from 0.34 to 0.43 e s^{-1}, or about 25%, and the power law exponent γ describing the decay of persistence with time flattens from 1.03 to 0.9, or about 13%, as the number of Omega cen exposure repeats increases from one to six. The other parameters in the fit, the ones that determine the "shape" of persistence, do not show a very systematic variation, although there may be a trend to a somewhat lower characteristic fluence x_o with larger numbers of repeats. In any event, these results imply that a full model of persistence in the WFC3/IR array

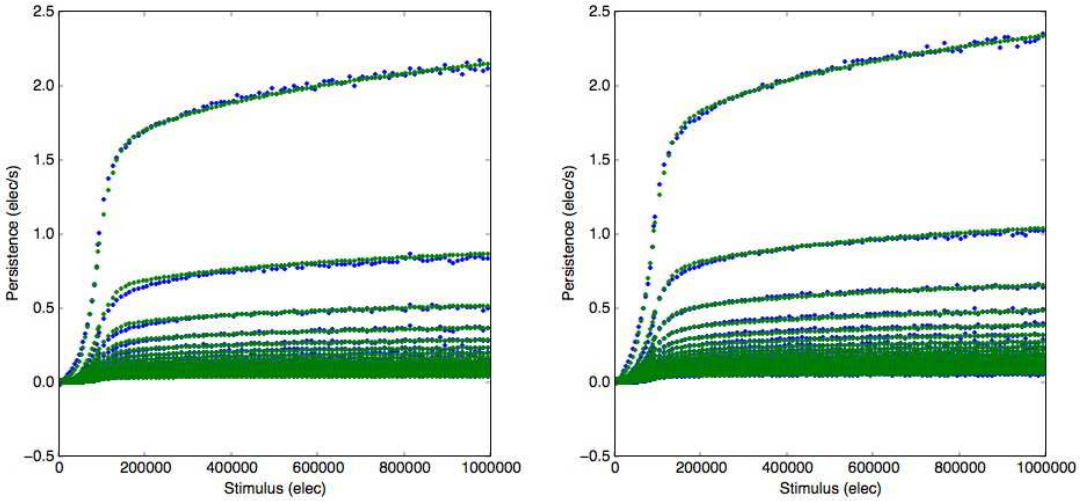

Figure 4. Examples of a model fits to the data from Visits 11 (left) and 26 (right). The observed values are plotted in blue; the fits are plotted in green.

must incorporate the complete exposure history.

We note in passing that the fitted parameters show some scatter, possibly more than one should expect from observation to observation. The derived amplitude from the model fits for the two visits with 3 (5) repeats differ by about 2% (4%), and the amplitude for visit 22 with 2 repeats is higher than for one of the visits with 3 repeats. This may be due in part due to the fact that different regions of the detector are saturated in the different visits. There is a gradual change in persistence amplitude across the face of the detector. On the other hand, there are no strong gradients in the density of stars bright enough to cause persistence at any of the the positions in Omega Cen that we observed, and, based on the tests we have done with tungsten lamp exposures, persistence does not show much structure on small scales. We have observed variations in persistence in nominally identical measurements involving tungsten lamp exposures. The experiments described here which start with an exposure of Omega Cen eliminate one source of non-repeatability, since variations in dark rate can be isolated from variations in persistence. But they have not (at least to date) allowed us to determine what causes variations in the persistence.

As mentioned above, the model we have used to characterize the persistence does not fit the knee of the persistence curve as well as it fits elsewhere. The problem is associated with both the shape of the persistence curve and its time history. To explore this, we have fit different power laws of the form

$$P = A\left(\frac{t}{1000\ s}\right) \tag{2}$$

as a function of fluence. If persistence were a separable function of fluence and time,

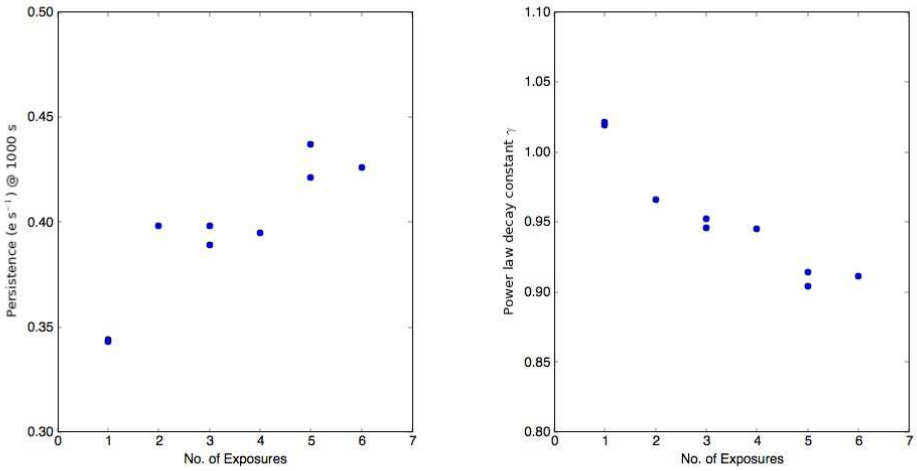

Figure 5. Amplitude and power law slopes derived from fits based on our initial model (Equation 1) as a function of the number of repeated exposures.

then this might be expected to provide a better functional form for persistence than the model we have used in the past.

The results are shown in Figure 6 for all of the visits at position 1. The results for other positions are similar. The general shape of the amplitude A is similar to the Fermi-like function we have used previously. However, within a single visit the power law decay is more rapid at lower fluence levels. Comparing different numbers of repeats, we see that the amplitude of persistence is higher for more repeats, and that, particularly at higher fluence levels, the persistence decay is characterized by a flatter slope.

The time decay of persistence cannot follow a power law at very short times, and may not follow it at very long times. However, it is interesting to ask the question of how much "equivalent charge" is released as a function of fluence during the period of time when measurements exist. This can be obtained by simply integrating the current released, that is the persistence, over the time interval of the measurements, or over whatever interval we believe our power law fits might apply, perhaps 100 to 10,000 s. This is shown in the left panel of Figure 7. As before, the blue, green, and red data points correspond to 1, 3, and 5 repeats, respectively. In terms of models of persistence involving traps, this suggests that there are about 1,000 traps that capture and release charge at a fluence level of 10^5 e for a 349 s exposure with no repeats.[2] For five repeats, there appear to be about 1,300 traps. The fact that more traps are filled in visits with five repeats is a consequence of finite trapping times.

[2]We use the word "equivalent charge" here, and we probably should use the words "equivalent number of traps" because persistence is measured as a drop in voltage, rather than in electrons directly. In the model of persistence outlined by Smith et al. (2008ab), the drop in voltage due to the release of an electron by a trap depends on the location of the trap.

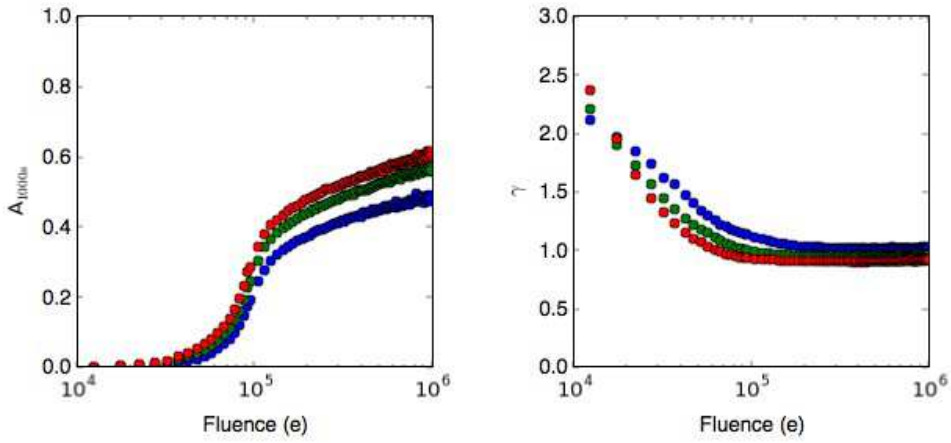

Figure 6. Power law fits to persistence as a function of fluence based on data from Position 1. The fitted amplitude at 1000 s is in the left hand panel and the fitted power law index γ is in the right. The blue, green and red data points correspond to the results for 1, 3, and 5 repeats, respectively.

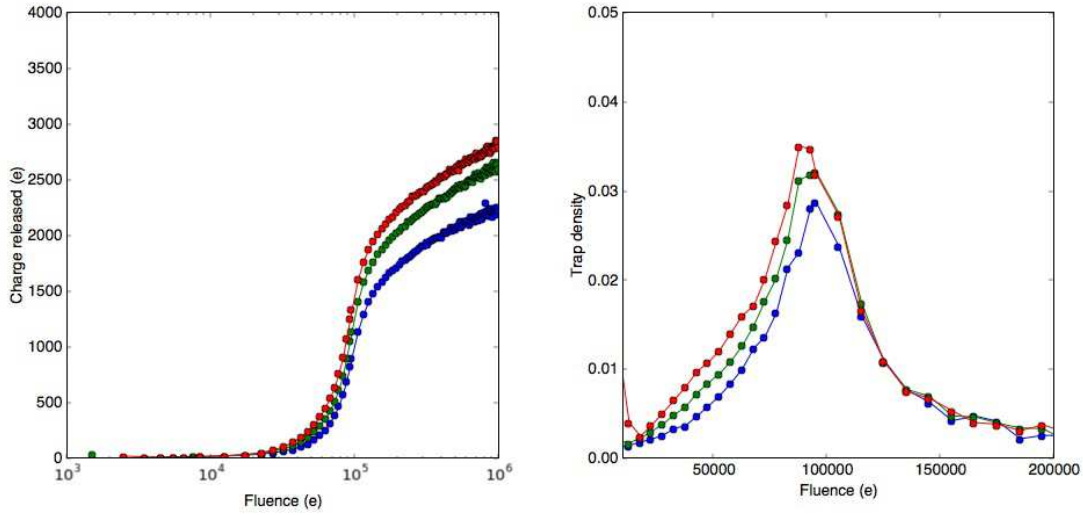

Figure 7. Left: The integral from 100 to 10,000 s of the current released as persistence for the 3 visits at position 1. Right: The ”effective” trap density measured as a function of fluence.

If traps were filled as soon as the fluence reached a certain value, one could differentiate the curves in the left panel of Figure 7 with respect to fluence to estimate the trap density (as a function of fluence). The analysis shows that trapping times are finite, but such a plot is still interesting as an approximate indication. The results are shown in right panel of Figure 7, in units of number of traps per electron.[3] If one knew the distribution of trapping times, one could use curves of this type to deduce the actual trap density. Finite trapping times would cause traps that should have appeared at a lower fluence level to show up at a higher fluence. Thus the actual density distribution of traps has more traps at lower fluence levels than appears to be the case in the figure, i.e., the curves are an underestimate of the trap density at low fluences. By this argument, this also suggests that the trap density at higher fluence is an overestimate.

In addition, at this point, we should remind ourselves that the analysis we have conducted here is based on the "flt" files, which do not reflect voltage levels in the detector pixels at high fluence levels nearly as accurately as the "raw" files. The primary reason to expect a bend in the persistence curve in the left panel of 7 is that once the detector is fully saturated, the "raw" pixel values do not increase much further, and the voltage levels within the diodes cease to change much. A physical model based on traps and voltage levels might well ascribe the bulk of the rise in persistence above a fluence of 100,000 electrons to finite trapping times. A way to explore this would be to carry out a series of observations of the type described here, but with different filters with very different band widths, requiring very different exposure times. One would expect that the amount of persistence at a fixed fluence level would increase with the length of the exposure, particularly at high fluence levels.

Summary

Our analysis of persistence due to varying numbers of exposures of fields in Omega Cen shows that the amplitude and duration of persistence are affected by the detailed exposure history of a pixel. The effects are relatively large: at 1000 s, for the exposure sequence chosen here, the amplitude of the persistence of a saturated pixel can vary by almost 0.1 e s^{-1}, depending on the number of un-dithered exposures. And while it is true that very few observations are carried out with un-dithered exposures, the results of the study presented here indicate with a high degree of confidence that one would see differences in persistence (for a given fluence level) depending on the overall length of a multiaccum observation.

At the present time, the WFC3 group provides an estimate of persistence in all WFC3 IR images, accessible to observers through the MAST archive. The estimate there is based on the model described in the Introduction. The parameters used are similar to those derived here for single repeats, with A of 0.4 e s^{-1} and γ of -1. Given that most science observations are dithered after individual exposures this is probably

[3]Formally, the quantity obtained by differentiating the charge released as persistence with respect to fluence, also measured in electrons, is dimensionless. To the extent that each electron released represents one trap, the units are effectively the number of traps per electron.

appropriate. We advise users that these estimates are to be used primarily for determining which pixels should be treated with suspicion during science analysis, and only secondarily for the subtraction of persistence. If users would like to subtract persistence from their science images they need to inspect the results carefully and possibly subtract scaled versions of the estimate that is provided.

On the other hand, the results from this study suggest a clear path forward toward a better model of persistence. The new model should 1) take into account that persistence is a function not simply of how much a pixel has been saturated in previous exposures by also the time it remained saturated, and 2) recognize that the rate at which persistence declines depends on the fluence.

Acknowledgements

We thank Bryan Hilbert for a careful reading of this manuscript.

References

Hilbert, B. & Petro, L. 2012, "WFC3/IR Dark Current Stability," WFC3 ISR 2012-11.

Long, K.S., Baggett S. M. & MacKenty, J. W. , 2013, "Characterizing Persistence in the WFC3 IR Channel: Finite Trapping Times," WFC3 ISR 2013-06

Long, K.S., Baggett, S.M., MacKenty, J.W., and Riess, A.G., 2012, "Characterizing persistence in the IR detector within the Wide Field Camera 3 instrument on the Hubble Space Telescope," Proceedings of the SPIE, 8442, 84421W-9

Smith, R.M., Zavodny, M., Rahmer, G. & Bonati, M., 2008a, "A theory for image persistence in HgCdTe photodiodes," Proceedings of the SPIE, 7021, 70210J-1

Smith, R. M., Zavodny, M., Rahmer, G., Bonati, M., 2008b, "Calibration of image persistence in HgCdTe photodiodes," Proceedings of the SPIE, 7021, 70210K-1